

In vivo targeting of lentiviral vectors pseudotyped with the Tupaia paramyxovirus H glycoprotein bearing a cell-specific ligand

Takele Argaw,¹ Michael P. Marino,¹ Andrew Timmons,¹ Lindsey Eldridge,¹ Kazuyo Takeda,² Pingjuan Li,^{1,3} Anna Kwilas,¹ Wu Ou,^{1,4} and Jakob Reiser¹

¹Division of Cellular and Gene Therapies, Center for Biologics Evaluation and Research, US Food and Drug Administration (FDA), Silver Spring, MD 20993, USA;

²Microscopy and Imaging Core Facility, Center for Biologics Evaluation and Research, FDA, Silver Spring, MD 20993, USA; ³Vedere Bio, Inc., Cambridge, MA 02139, USA

Despite their exceptional capacity for transgene delivery *ex vivo*, lentiviral (LV) vectors have been slow to demonstrate clinical utility in the context of *in vivo* applications. Unresolved safety concerns related to broad LV vector tropism have limited LV vectors to *ex vivo* applications. Here, we report on a novel LV vector-pseudotyping strategy involving envelope glycoproteins of Tupaia paramyxovirus (TPMV) engineered to specifically target human cell-surface receptors. LV vectors pseudotyped with the TPMV hemagglutinin (H) protein bearing the interleukin (IL)-13 ligand in concert with the TPMV fusion (F) protein allowed efficient transduction of cells expressing the human IL-13 receptor alpha 2 (IL-13R α 2). Immunodeficient mice bearing orthotopically implanted human IL-13R α 2 expressing NCI-H1299 non-small cell lung cancer cells were injected intravenously with a single dose of LV vector pseudotyped with the TPMV H-IL-13 glycoprotein. Vector biodistribution was monitored using bioluminescence imaging of firefly luciferase transgene expression, revealing specific transduction of tumor tissue. A quantitative droplet digital PCR (ddPCR) analysis of lung tissue samples revealed a >15-fold increase in the tumor transduction in mice treated with LV vectors displaying IL-13 relative to those without IL-13. Our results show that TPMV envelope glycoproteins can be equipped with ligands to develop targeted LV vectors for *in vivo* applications.

INTRODUCTION

A number of strategies aimed at broadening the tropism of gene-therapy vectors to transduce previously nonpermissive cells or to replace a vector's tropism to transduce specific target cells exclusively have been described.^{1,2} For example, the host range of retroviral vectors, including that of lentiviral (LV) vectors, can be expanded or altered by a process known as pseudotyping. Pseudotyped retroviral vector particles bear envelope (Env) glycoproteins derived from other enveloped viruses and acquire the tropism of the virus from which the glycoprotein was derived.³ Although targeting strategies for LV vectors involving the traditional pseudotyping approach are well established,³⁻⁵ it has been challenging to design LV vectors with a reduced tropism for the natural receptor and an increased specificity for a cho-

sen receptor to allow targeted transduction of specific cell types *in vitro* and *in vivo*. This is due to a number of issues, including low vector titers and a general lack of specificity of the strategies tested.^{2,6}

Over the past several years, a versatile strategy for LV vector targeting involving engineered measles virus (MV) hemagglutinin (H) and fusion (F) glycoproteins has emerged.⁵⁻⁷ The native MV H protein mediates attachment of the virus to CD46, signaling lymphocyte-activation molecule (SLAM),^{8,9} or Nectin-4¹⁰ on the cell surface and signals to the F protein to trigger cell fusion. The steps required to retarget this cell fusion reaction are ablation of H protein-mediated CD46, SLAM, and Nectin-4 receptor recognition and introduction of a new binding specificity in the H glycoprotein.^{5,7} Various ligands, including epidermal growth factor (EGF)¹¹, interleukin (IL)-13¹², single-chain antibodies,¹³ and designed ankyrin repeat proteins (DARPs),¹⁴ have been successfully displayed using MV H, allowing retargeted LV vector delivery. However, the high prevalence of antibodies against MV may hamper the efficacy of MV-derived therapeutics, including pseudotyped LV vectors containing MV glycoproteins, in a clinical setting due to vaccination or natural infection.¹⁵

Glycoproteins from other members of the *Paramyxoviridae* family, including those from the Tupaia paramyxovirus (TPMV), have also been used to pseudotype LV vectors.⁷ TPMV was originally isolated from a tree shrew (*Tupaia belangeri*)¹⁶ and has garnered particular interest in gene therapy due to its restrictive tropism. Indeed, TPMV is restricted to Tupaia cells, and no serological cross-reactivity with other *Paramyxoviridae* has been observed.¹⁶ The TPMV genome and the H and F proteins have been characterized extensively,^{17,18} revealing that receptor binding limits TPMV entry into other mammalian cells.¹⁹ The absence of pre-existing tropism for human

Received 5 November 2020; accepted 21 April 2021;
<https://doi.org/10.1016/j.omtm.2021.04.012>.

⁴Deceased

Correspondence: Jakob Reiser, Division of Cellular and Gene Therapies, Center for Biologics Evaluation and Research, FDA, 10903 New Hampshire Avenue, Building 52/72, Room 3106, Silver Spring, MD 20993, USA.

E-mail: jakob.reiser@fda.hhs.gov



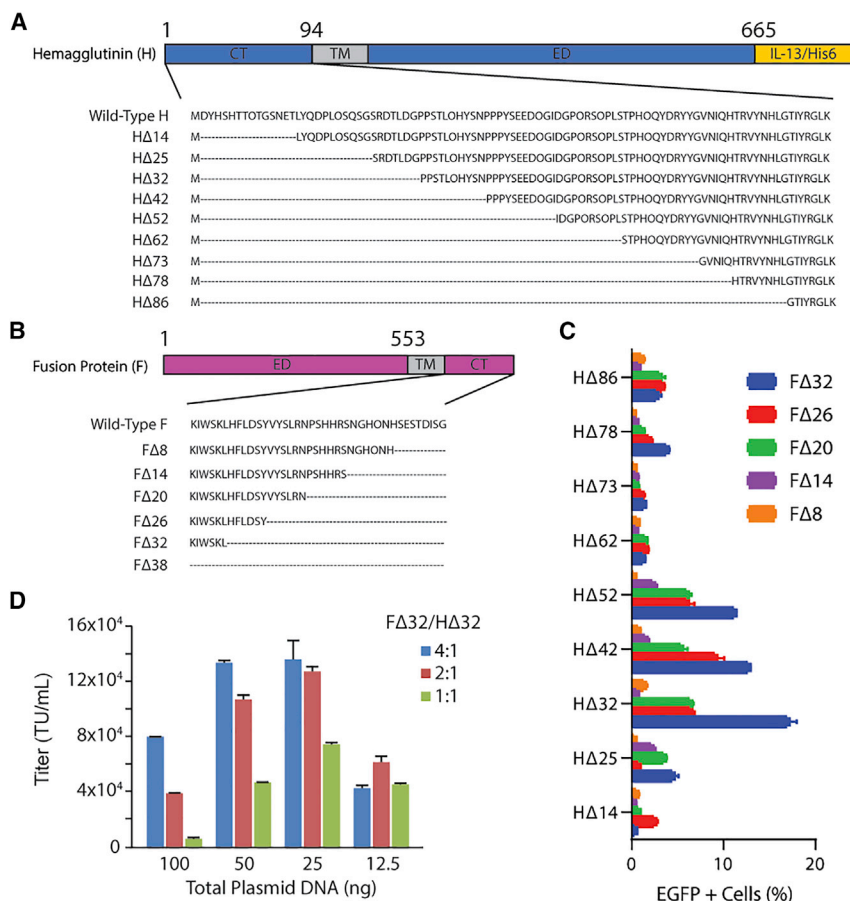


Figure 1. Pseudotyping LV vectors bearing engineered TPMV H and F glycoproteins

(A) Wild-type H protein and H protein variants bearing truncated CT sequences. IL-13 and 6-His-encoding sequences were added at the end of the extracellular domain (ED). (B) Wild-type F protein and F protein variants bearing CT truncations. (C) Transduction efficiency in U251 cells of un-concentrated EGFP-encoding NL(CMV)EGFP(CMV)/WPREDU3 LV vectors pseudotyped using various H-IL-13 protein variants in conjunction with various F protein variants (n = 2). (D) Optimization of the production of LV vectors bearing the TPMV HΔ32-IL-13 and FΔ32 glycoproteins. The titers of un-concentrated NL(CMV)EGFP(CMV)/WPREDU3 LV vectors pseudotyped with the FΔ32 and HΔ32-IL-13 glycoproteins in U251 cells are shown. The ratios and total amounts of the FΔ32 and HΔ32-IL-13 glycoprotein-encoding plasmid DNAs were varied during vector production (n = 2). Error bars represent mean ± standard error.

enhanced capacity to transduce human cells expressing IL-13Rα2. With the use of a variety of approaches, including immunohistochemistry and quantitative PCR, we demonstrate that TPMV glycoproteins can be used to design and create targeted and cell-specific LV vector pseudotypes.

RESULTS

Assessing pseudotyping efficiency of LV vectors bearing engineered TPMV glycoproteins

To optimize the efficiency of engineered TPMV-derived H and F glycoproteins to pseudotype LV vectors, a series of TPMV H and F protein variants with truncated cytoplasmic tails (CTs) were prepared and tested.

The TPMV H protein is a type II membrane protein consisting of 665 amino acids, including a CT of 94 amino acids¹⁷ (Figure 1A). Starting with a codon-optimized TPMV H protein coding region, we generated nine different TPMV H protein variants lacking 14, 25, 32, 42, 52, 62, 73, 78, and 86 amino acids, respectively, at the N terminus of the protein. The corresponding protein constructs are referred to as HΔ14, HΔ25, HΔ32, HΔ42, HΔ52, HΔ62, HΔ73, HΔ78, and HΔ86, respectively (Figure 1A). To direct LV vector transduction to IL-13Rα2-expressing cells, an IL-13-encoding sequence was added to the C-terminal ends of the various H protein constructs (Figure 1A).

The TPMV F protein is a 553-amino acid type I membrane protein¹⁷ bearing a 38-amino acid CT¹⁸ (Figure 1B). A codon-optimized F protein-encoding region was prepared, and CT-truncated variants of the F protein lacking 32, 26, 20, 14, and 8 amino acids from the C terminus, respectively, were prepared. These variants are referred to as FΔ32, FΔ26, FΔ20, FΔ14, and FΔ8, respectively (Figure 1B).

The pseudotyping efficiency of LV vectors bearing various combinations of the TPMV H-IL-13 and F protein variants was tested by

cells positions TPMV glycoproteins as attractive candidates for the design of specific and directed LV vector-pseudotyping strategies.

Few studies have been conducted to explore the potential of TPMV glycoproteins in modifying gene-delivery vectors. Single-chain variable fragments (scFvs) attached to TPMV H were used to target TPMV vectors to carcinoembryonic antigen in HEK293T cells¹⁹ and to EGF receptor (EGFR) and CD20 in human and African green monkey kidney cell lines.²⁰ In addition, TPMV-H-pseudotyped LV vectors displaying an anti-CD20 scFv were shown by Enkirch et al.²¹ to specifically target CD20 expressing human cells *in vitro*.

The purpose of this work was to investigate the *in vivo* specificity of TPMV glycoprotein-pseudotyped LV vectors bearing a ligand (IL-13) specific for human IL-13 receptor alpha 2 (IL-13Rα2). IL-13Rα2 binds IL-13 with high affinity²² and is overexpressed in a variety of human cancer cells.²³ In this study, we tested LV vectors pseudotyped with a modified TPMV H-glycoprotein displaying the IL-13 ligand in concert with a modified version of the TPMV F glycoprotein to target IL-13Rα2 expressing human non-small cell lung cancer (NSCLC) NCI-H1299 cells²⁴ xenografted into the lungs of NOD-scid IL-2Rγ^{null} (NSG) mice. The data obtained show that LV vectors pseudotyped with TPMV glycoproteins bearing the IL-13 ligand show an

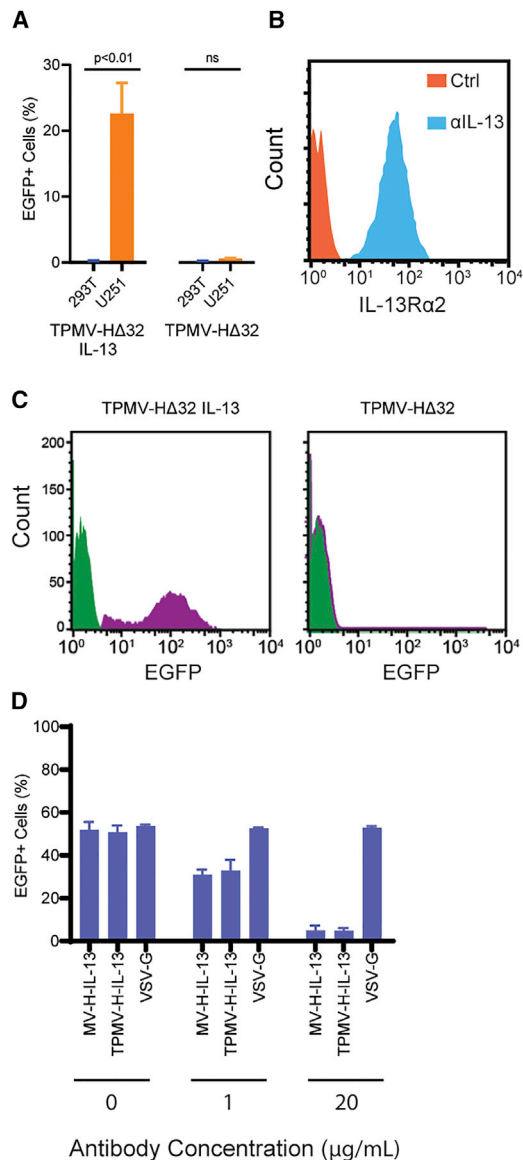


Figure 2. Specificity of *in vitro* transduction of LV vectors bearing engineered TPMV glycoproteins

(A) Transduction of U251 and HEK293T cells using unconcentrated LV vectors pseudotyped with TPMV H Δ 32 IL-13/F Δ 32 or H Δ 32/F Δ 32 glycoproteins ($n = 2$). (B) Analysis of IL-13R α 2 levels in NCI H1299 cells. Cells were incubated with goat anti-human IL-13-R α 2 antibody (referred to as α IL-13) and a fluorescein isothiocyanate (FITC)-labeled secondary antibody. A polyclonal goat antibody was used as a control (Ctrl). (C) Transduction of NCI H1299 cells using concentrated EGFP-encoding LV vectors bearing TPMV H Δ 32 IL-13/F Δ 32 (left panel) or TPMV H Δ 32/F Δ 32 glycoproteins (right panel). The areas highlighted in green represent untransduced cells. (D) NCI-H1299 cells treated with a goat anti-IL-13R α 2 polyclonal antibody before and during transduction. Concentrated LV vectors pseudotyped using the TPMV H Δ 32 IL-13 plus F Δ 32 glycoproteins (MOI = 4), the measles virus (MV) Hc Δ 18-AA-IL-13 plus Fc Δ 30 glycoproteins¹² (MOI = 4), or VSV-G (MOI = 0.2) were used ($n = 2$). Error bars represent means \pm standard error.

transducing IL-13R α 2-expressing U251 glioblastoma cells.² To do this, the pNL(CMV)EGFP/CMV/WPRE Δ U3 LV vector plasmid that we previously described¹² was used. Figure 1C shows that the EGFP-encoding NL(CMV)EGFP/CMV/WPRE Δ U3 LV vector pseudotyped using the H Δ 32-IL-13 variant in conjunction with the F Δ 32 variant produced the highest vector titers. The H Δ 32-IL-13 and H Δ 32 variants and the F Δ 32 glycoprotein variants were used in all subsequent experiments.

To optimize the production of LV vectors bearing the TPMV H Δ 32-IL-13 and F Δ 32 glycoproteins, the ratios of the F Δ 32 and H Δ 32-IL-13 glycoprotein-encoding plasmids and the total amount of plasmid DNA used during vector production were investigated. As shown in Figure 1D, a plasmid ratio of 4:1 yielded the highest vector titers using a total of 100, 50, and 25 ng of the two plasmid DNAs, whereas at lower total amounts (12.5 ng) of the two plasmids, a 2:1 ratio was better.

As indicated in Figure 1A, the TPMV H Δ 32-IL-13 glycoprotein bears a six-histidine tag at the C terminus. The six-histidine tag may promote the transduction by LV vectors pseudotyped with these glycoproteins of cells containing the α His pseudoreceptor²⁵ as demonstrated before for TPMV vectors.²⁰ The results presented in Figure S1 show that Vero- α His cells²⁵ were transduced efficiently using LV vectors containing the TPMV H Δ 32-IL-13 glycoprotein or TPMV H Δ 32 (lacking IL-13), whereas Vero cells lacking the α His pseudoreceptor were not. This result indicates that transduction of Vero- α His cells was mediated by the six-histidine tag and the α His pseudoreceptor. With the use of this assay, the transduction efficiencies of TPMV H Δ 32-IL-13 and TPMV H Δ 32 pseudotypes were similar, indicating that glycoprotein incorporation levels in vector particles were similar for the two pseudotypes.

Table S1 shows the results of three independent batches of TPMV H Δ 32-IL-13/F Δ 32- or TPMV H Δ 32/F Δ 32-pseudotyped LV vectors produced using HYPERFlask vessels and concentrated using Mustang Q^{26,27} or Sartobind Q membrane adsorbers. The titers for concentrated TPMV H Δ 32-IL-13/F Δ 32 pseudotypes were up to 1×10^7 transduction units (TU)/mL, a value similar to that reported previously for concentrated LV vectors pseudotyped using MV H and F glycoproteins.²⁷

Analysis of the *in vitro* cell tropism of the LV vector bearing engineered TPMV glycoproteins

We next wanted to confirm that transduction of IL-13R α 2-expressing cells by LV vectors pseudotyped with the TPMV H Δ 32-IL-13 and F Δ 32 glycoproteins was specific. To do this, U251 cells were transduced with the EGFP-encoding NL(CMV)EGFP/CMV/WPRE Δ U3 LV vector pseudotyped with the TPMV H Δ 32-IL-13/F Δ 32 or H Δ 32/F Δ 32 glycoproteins. The results presented in Figure 2A show that the percentage of EGFP-positive U251 cells in the absence of the IL-13 ligand was considerably lower compared to cells transduced with vectors containing IL-13. HEK293T cells that do not express IL-

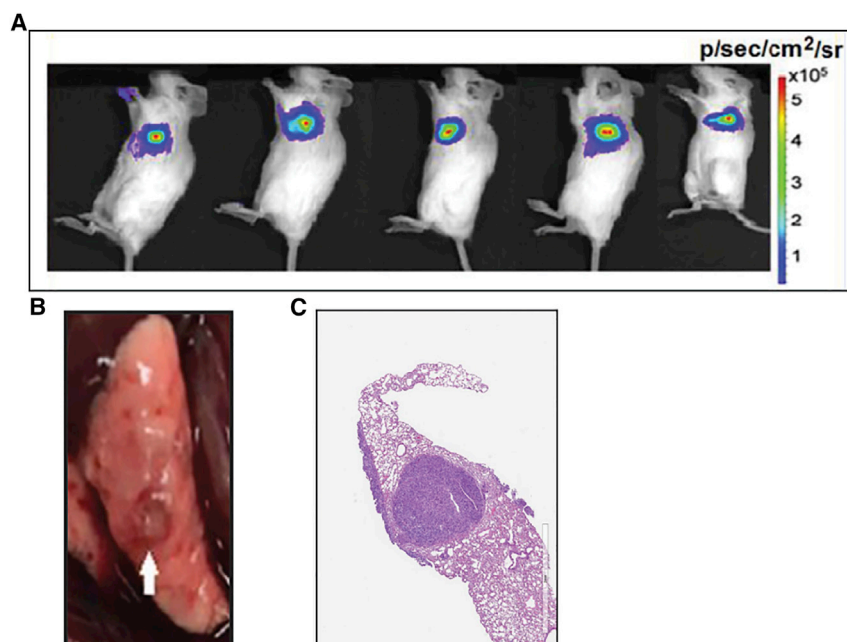


Figure 3. Orthotopic lung cancer model to evaluate *in vivo* targeting of LV vectors

(A) *In vivo* bioluminescence imaging of mice 4 weeks after intrathoracic injection of NCI-H1299 GLuc cells (1.5×10^6). Two experiments, with 6 to 7 mice each, were performed. (B) Representative macroscopic view of a lung lobe bearing a tumor nodule (white arrow). Animals were sacrificed 42 days post-cell engraftment. (C) Microscopic view after H&E staining of a lung section 6 weeks post-cell engraftment.

13R α 2 did not reveal any EGFP-positive cells, independent of IL-13 (Figure 2A).

These findings were confirmed in the context of the NCI-H1299 human NSCLC cell line that expresses IL-13R α 2 (Figure 2B). IL-13R α 2 levels in NCI-H1299 cells were comparable to those observed in U251 cells (T.A., unpublished data). Efficient transduction of NCI-H1299 cells was dependent on the presence of the IL-13 ligand (Figure 2C, left panel); Vectors lacking the IL-13 ligand revealed transduction efficiencies at background levels (Figure 2C, right panel).

In a subsequent experiment, IL-13R α 2-expressing NCI-H1299 cells were treated with a polyclonal goat anti-IL-13R α 2 antibody 1 h before and during transduction. Figure 2D shows that transduction was blocked in a dose-dependent manner for vectors pseudotyped with TPMV or MV H and F glycoproteins but not for vectors pseudotyped with vesicular stomatitis virus G protein (VSV-G). Taken together, these results are consistent with the view that transduction of U251 and NCI-H1299 cells by LV vectors bearing TPMV H Δ 32-IL-13/F Δ 32 glycoproteins was mediated by IL-13 and IL-13R α 2.

Orthotopic lung cancer model to evaluate targeting of LV vectors bearing TPMV glycoproteins

To investigate the targeting specificity *in vivo* of LV vectors bearing TPMV H Δ 32-IL-13/F Δ 32 or H Δ 32/F Δ 32 glycoproteins, a mouse-based orthotopic lung cancer model involving NCI-H1299 NSCLC cells was established.²⁸ To assess tumor formation, NCI-H1299 cells were tagged using a membrane-bound version of Gaussia luciferase (GLuc).¹² The tagged cells are referred to as NCI-H1299 GLuc cells. NCI-H1299 GLuc cells (1.5×10^6) were implanted into the left lungs of NSG mice via intrathoracic injection,²⁹ and tumor formation was

evaluated by bioluminescence imaging after injection of the GLuc substrate coelenterazine at various time points. The results obtained showed that NCI-H1299 GLuc cells xenografted intrathoracically produced a bioluminescent signal within 2 weeks after cell injection; up to 90% of the animals revealed tumors 4 to 5 weeks post-cell injection (T.A., unpublished data), resulting in a strong bioluminescence signal in the left lobes of the lungs (Figure 3A). For macroscopic examination of tumors and histopathological analysis of lung lesions, animals were sacrificed 5.5 weeks post-intrathoracic cell injection. Lung tissue was processed for hematoxylin and eosin (H&E) staining and immunohistochemical (IHC) analysis. The macroscopic examination typically revealed one or two tumor nodules in injected lungs. No tumor nodules were seen in uninjected lungs or in distant organs such as liver, spleen, and major lymph nodes (T.A., unpublished data). Figure 3B shows a tumor nodule grown in the parenchyma of the lung of a mouse sacrificed 5.5 weeks post-implantation of NCI-H1299 GLuc cells. Figure 3C shows a representative H&E staining of a tumor nodule grown in the parenchyma of the lung of a mouse sacrificed 5.5 weeks post-cell implantation.

Overall, these results confirmed that the GLuc signal observed by bioluminescence imaging after injection of the coelenterazine substrate reflected tumor formation by NCI-H1299 GLuc cells at the site of cell implantation.

Analysis of the *in vivo* cell tropism of the LV vector bearing engineered TPMV glycoproteins

To assess LV vector distribution *in vivo*, pseudotyped vector particles were injected intravenously (i.v.) into tumor-bearing mice 4 weeks after NCI-H1299 GLuc cell implantation (Figure 4A). The NL(CMV)TK2ALuc2/CMV/WPRE Δ U3 LV vector encoding the herpes simplex virus-1 thymidine kinase (HSV-1 TK) SR39 mutant protein,³⁰ a F2A peptide, and firefly luciferase (FLuc) (Figure 4B) was used.

Vector distribution was assessed 7 days later by whole-body bioluminescence imaging after injection of the FLuc substrate D-luciferin (Figure 4C). Mice injected with the NL(CMV)TK2ALuc2/CMV/WPRE Δ U3 vector pseudotyped with the TPMV H Δ 32-IL-13/F Δ 32 glycoproteins produced a bioluminescent signal (Figure 4C, left

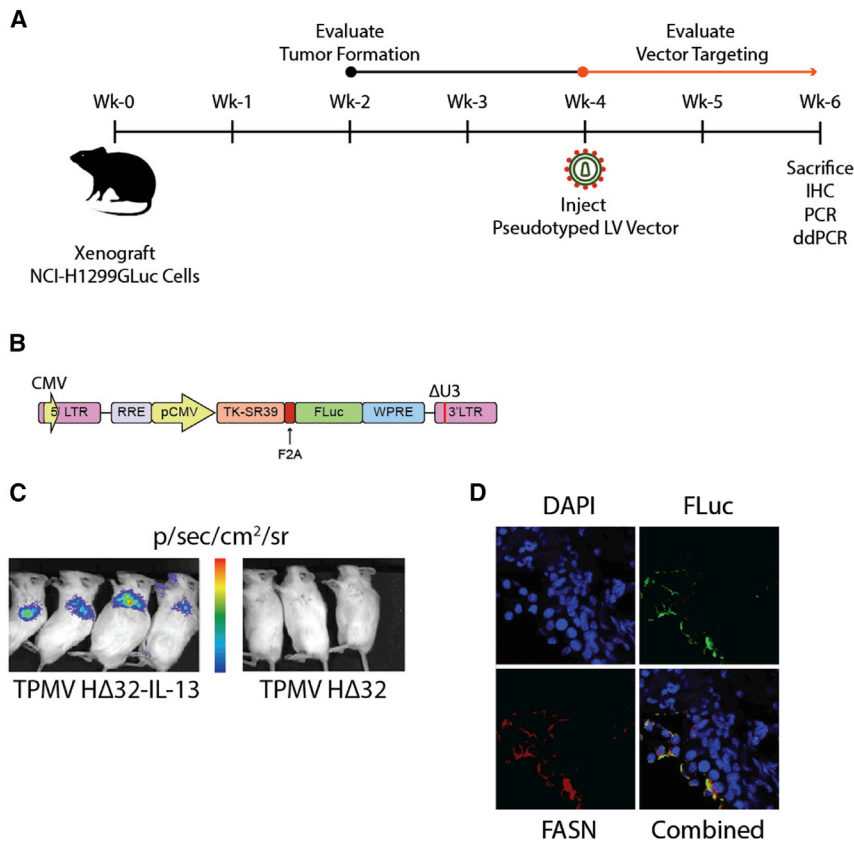


Figure 4. Analysis of *in vivo* cell tropism of LV vectors bearing engineered TPMV glycoproteins

(A) Outline of lung cancer model used to assess LV vector targeting. (B) Outline of the NL(CMV)TK2ALuc2/CMV/WPREΔU3 LV vector used *in vivo*. (C) Bioluminescence imaging of tumor-bearing animals 7 days post *i.v.* injection of NL(CMV)TK2ALuc2/CMV/WPREΔU3 LV vectors (42 days post-cell engraftment). Left panel: vectors pseudotyped with TPMV HΔ32-IL-13; right panel: vectors pseudotyped with TPMV HΔ32 lacking IL-13. (D) Co-localization of vector-encoded FLuc and the human cell-specific marker FASN. Top left panel: DAPI staining; top right panel: anti-FLuc staining; bottom left panel: anti-FASN staining; bottom right panel: picture combining all three panels. Animals were sacrificed 42 days post-cell engraftment (7 days after LV vector injection), and lung tissue samples were collected and processed for immunohistochemistry.

panel), whereas LV vectors pseudotyped with TPMV HΔ32 lacking the IL-13 ligand did not (Figure 4C, right panel). Also, mice lacking tumors injected with TPMV HΔ32-IL-13/FΔ32-pseudotyped NL(CMV)TK2ALuc2/CMV/WPREΔU3 vectors did not reveal a bioluminescence signal (Figure S2). These results indicate that LV vectors pseudotyped with TPMV HΔ32-IL-13 had a strong target preference, whereas TPMV HΔ32 vectors lacking IL-13 did not successfully transduce the target cells.

To investigate vector-targeting events more directly, lung sections were prepared and analyzed using immunohistochemistry. Vector-encoded FLuc was detected using a monoclonal anti-FLuc antibody and an Alexa Fluor 488-tagged secondary antibody (Figure 4D, upper right and bottom right panels; Figure S3B). Lung sections from tumor-bearing animals without LV vector injection did not reveal an immunofluorescence signal above background after staining using a monoclonal anti-FLuc antibody and an Alexa Fluor 488-tagged secondary antibody (Figure S3C), whereas lung tumor sections from a mouse that was *i.v.* injected with the NL(CMV)TK2ALuc2/CMV/WPREΔU3 LV vector (Figure S3D) did, indicating that the anti-FLuc staining observed was specific.

Human cells were identified using a monoclonal antibody directed against human fatty acid synthase (FASN) and an Alexa Fluor 645-tagged secondary antibody (Figure 4D, lower left and lower right

panels). Co-localization of FLuc-positive and FASN-positive cells (Figure 4D, lower right panel) indicates the presence of LV vector-transduced NCI-H1299 cells. This conclusion is supported by the colocalization analysis of *in vivo*-transduced cells (presented in Figure S4).

Analysis of *in vivo*-transduced cells by PCR and droplet digital PCR (ddPCR)

The presence of LV vector sequences in lung tissue samples was determined by PCR using primers specific for HSV-1 TK transgene and hRNaseP genomic sequences. To do this, genomic DNA from lung tumor samples collected from tumor-bearing animals injected with NL(CMV)TK2ALuc2/CMV/WPREΔU3 LV vectors pseudotyped with the TPMV HΔ32-IL-13/FΔ32 or TPMV HΔ32/FΔ32 glycoproteins was used. The results obtained showed that genomic DNA extracted from lung samples of animals injected with TPMV HΔ32-IL-13/FΔ32-pseudotyped vectors produced an HSV-1 TK transgene-specific PCR product (Figure 5A, top left panel), whereas genomic DNAs from lung samples of animals injected with TPMV HΔ32/FΔ32-pseudotyped vectors did not (Figure 5A, top right panel). With the use of hRNaseP-specific primers, all samples produced a PCR fragment of the expected size (Figure 5A, bottom panels).

We next conducted a ddPCR analysis to determine vector-specific HSV-1 TK transgene sequences and human and mouse prostaglandin E receptor2 (PTGER2) sequences³¹ in genomic DNA extracted from mouse lung samples. The specificity of the primers and probes used for ddPCR was assessed using genomic DNA from human NCI-H1299 cells, mouse NIH 3T3 cells, and mouse lung tissue. Figure 5B shows that the PTGER2 primers and probes used were able to distinguish between human and mouse sequences and that there were no TK-specific sequences present in genomic DNA obtained from NCI-H1299 or NIH 3T3 cells or mouse lung tissue.

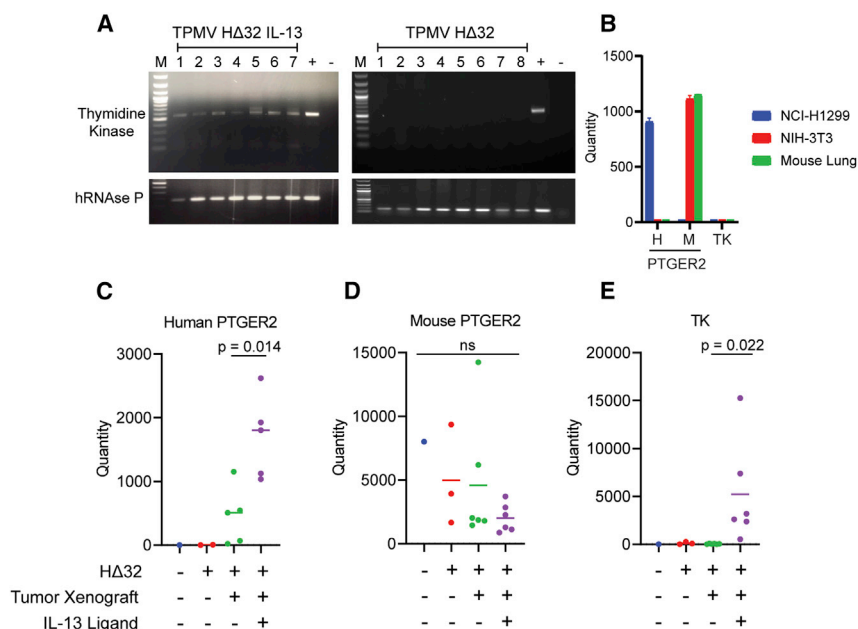


Figure 5. Analysis of *in vivo*-transduced cells by PCR and ddPCR

(A) PCR analysis of HSV-1 TK transgene and hRNaseP genomic sequences in lung samples collected from animals injected with NL(CMV)TK2ALuc2/CMV/WPREΔU3 LV vectors containing the TPMV glycoproteins. Top panel: PCR analysis involving HSV-1 TK primers. Left part: genomic DNA from lungs of animals injected with vectors pseudotyped with TPMV HΔ32-IL-13; right part: vectors pseudotyped with TPMV HΔ32 lacking IL-13. Bottom panel: PCR analysis involving hRNaseP primers. Left part: genomic DNA from lungs of animals injected with vectors pseudotyped with TPMV HΔ32-IL-13; right part: vectors pseudotyped with TPMV HΔ32 lacking IL-13. (+) and (-) refer to PCR reactions conducted using NL(CMV)TK2ALuc2/CMV/WPREΔU3 plasmid DNA or no plasmid DNA. (B) Performance of the human PTGER2, mouse PTGER2, and TK ddPCR assays on genomic DNA isolated from NCI-H1299 cells, NIH 3T3 cells, or mouse lung tissue. (C) ddPCR-based quantification of human PTGER2 sequences. (D) ddPCR-based quantification of mouse PTGER2 sequences. (E) ddPCR-based quantification of HSV-1 TK transgene sequences. Error bars represent means \pm standard error.

Genomic DNA extracted from tumor biopsies was analyzed next. In all samples, human PTGER2, mouse PTGER2, and vector-specific TK sequences were quantified. In mice-bearing tumor xenografts, we observed a statistically significant increase in human PTGER2 sequences in animals that were treated with the LV vector containing the IL-13 ligand compared to animals treated with a LV vector lacking IL-13, possibly due to IL-13 vector-induced agonism of the IL-13R α 2 on the xenografted tumor²⁴ (Figure 5C). No increase was observed in mouse PTGER2 sequences (Figure 5D). Encouragingly, we observed minimal vector-specific TK sequences in biopsies taken from mice treated with the non-IL-13-containing LV vector. However, we observed a substantial increase in vector-specific TK sequences in biopsies taken from mice treated with the IL-13-containing LV vector (Figure 5E).

DISCUSSION

LV vectors have been used in numerous clinical trials to introduce transgene sequences into hematopoietic stem cells and mature T cells *ex vivo*.^{32,33} Four LV vector-based gene-therapy products have recently received regulatory approval, including Kymriah (tisagenlecleucel) for the treatment of relapsed/refractory B cell acute lymphoblastic leukemia (B-ALL),³⁴ Zynteglo (betibeglogene autotemcel) for the treatment of transfusion-dependent beta-thalassemia,³⁵ Breyanzi (lisocabtagene maraleucel) for the treatment of relapsed or refractory large B cell lymphoma (LBCL),³⁶ and Abecma (idecabtagene vicleucel) for the for the treatment of adult patients with relapsed or refractory multiple myeloma.³⁷

LV vectors are also being applied directly *in vivo* for therapeutic purposes. A non-primate LV vector system based on equine infectious anemia virus (EIAV) has been investigated clinically to treat ocular disorders.³⁸ In another *in vivo* application, an HIV-1-based, integra-

tion-deficient LV vector expressing the New York esophageal squamous cell carcinoma 1 (NY-ESO-1) cancer testis antigen and targeted to dendritic cells was used to promote an immune response against NY-ESO-1-expressing tumors.³⁹

In vivo gene-therapy approaches involving LV vectors have faced a number of challenges, including efficiency of transgene delivery; a need for tissue-restricted transgene expression; immunogenicity to both the product encoded by the transgene as well as components of the vector, including its envelope; and inactivation by the human complement cascade. Surface engineering approaches will be critical to help mitigate some of these issues.⁵

This report describes a novel pseudotyping system for LV vectors involving the TPMV H and F glycoproteins allowing targeting of LV vectors to specific receptors. Despite the phylogenetic relationship between TPMV and human pathogens, no serological cross-reactivity with other *Paramyxoviridae* has been observed.¹⁶ The likely absence of TPMV-reactive antibodies in human subjects has resulted in efforts toward the development of TPMV-pseudotyped LV vectors for gene-therapy applications.²¹

One of the challenges for using LV vectors bearing paramyxovirus-derived glycoproteins is low titer during vector production. This results in the need to manufacture large volumes of the vectors and to concentrate them to appropriate titers. Previously, we adapted an anion-exchange membrane chromatography method to concentrate MV glycoprotein-pseudotyped LV vectors.²⁷ With the use of the same anion-exchange membrane chromatography approach to concentrate TPMV-pseudotyped LV vectors in conjunction with the use of HYPERFlask vessels during vector production,²⁶ titers up to 1×10^7 TU/mL were obtained. These titers compare favorably

to those obtained using LV vectors pseudotyped with receptor-targeted Nipah virus glycoproteins.⁴⁰ Compared to the titers of LV vectors pseudotyped with VSV-G, the titers of LV vectors pseudotyped with TPMV H and F glycoproteins were lower, typically by at least two logs (M.P.M., unpublished data).

Our work has focused on IL-13-displaying LV vectors bearing TPMV glycoproteins to target IL-13R α 2-expressing cells. To optimize this system, we tested a number of H and F protein variants containing CT truncations for their ability to mediate transgene delivery into IL-13R α 2-expressing U251 cells. An F protein variant with a six-amino acid CT (F Δ 32) resulted in the highest vector titers. This finding agrees with results obtained involving a CD20-targeted LV vector containing TPMV glycoproteins.²¹ For the TPMV H-IL-13 protein, we found that the H Δ 32 protein variant fused to IL-13 produced the highest vector titers. This is in contrast to the findings obtained by Enkirch et al.,²¹ which showed that the TPMV H Δ 80 variant in conjunction with an anti-CD20 single-chain antibody produced the highest vector titers in HT1080-CD20 cells. The reason for this discrepancy is not known. However, it may be due to differences in the targeting ligand used and its biophysical properties.⁴¹

The results presented in this paper show that IL-13R α 2-expressing human cells can be targeted *in vivo* upon systemic vector injection. Our findings are consistent with the view that transduction was mediated by the IL-13 ligand since LV vectors lacking IL-13 failed at transducing cells *in vitro* and *in vivo*. In NSG mice bearing xenografts of human lung tumor tissue, we were able to demonstrate the accumulation of vector-specific TK sequences in tumor biopsy samples. With the use of ddPCR, we quantified human PTGER2 sequences, mouse PTGER2 sequences, and vector-specific TK sequences in genomic DNA isolated from tumor biopsies taken from mice treated with TPMV H-pseudotyped LV vectors lacking IL-13 or LV vectors pseudotyped with TPMV H glycoproteins displaying IL-13. In mice treated with TPMV H-pseudotyped LV vectors lacking IL-13, we observed no accumulation of vector-specific TK sequences in tumor biopsies. However, in mice treated with LV vectors containing IL-13, we observed accumulation of vector-specific TK sequences in tumor biopsy samples. Given the small biopsy size and the complexity of working with xenografted solid tumors, we were unable to preemptively separate human and mouse tissues before performing genomic DNA isolations. However, we were able to quantify the composition of this heterogeneous population in terms of human gene sequences, mouse gene sequences, and vector-specific sequences.

A number of recent studies used surface-engineered LV vectors involving engineered MV glycoproteins to target specific cells *in vivo* following systemic vector injection, including liver sinusoidal and artery endothelial cells using CD105-targeted vectors⁴² and human CD4⁺ T cells using CD4-targeted LV vectors.^{43,44} CD4-targeted LV vectors may ultimately allow the *in vivo* generation of CD4⁺ chimeric antigen receptor (CAR) T cells for clinical applications. The capacity

of LV vector pseudotypes involving CD4-targeted TPMV glycoproteins to target CD4⁺ T cells *in vivo* remains to be determined.

MATERIALS AND METHODS

Plasmid constructs

The pNL(CMV)EGFP/CMV/WPRE Δ U3 LV vector plasmid was described before.¹² It is available through Addgene (plasmid #41970). The pNL(CMV)TK2ALuc2/CMV/WPRE Δ U3 LV vector plasmid was derived from the pNL(CMV)EGFP/CMV/WPRE Δ U3 plasmid¹² by replacing the EGFP coding region with a codon-optimized sequence encoding the HSV-1 TK SR39 mutant protein³⁰ (Geneart AG, Regensburg, Germany), a F2A sequence, and a FLuc-encoding sequence.¹² It is available through Addgene (plasmid #163965).

Synthetic, codon-optimized versions of the TPMV H and F protein coding regions (GenBank: AF079780.2) were prepared by GenScript (Piscataway, NJ, USA). The pCG-Hc Δ 18-AA-IL-13 plasmid¹² was used as a backbone with the TPMV H and F coding regions replacing the Hc Δ 18-AA-IL-13 sequence.

TPMV H protein variants bearing N-terminal truncations were generated by replacing the 5' end of the H protein coding region with PCR fragments containing the corresponding deletions. TPMV F protein variants bearing C-terminal truncations were generated similarly by replacing the 3' end of the F protein coding regions with PCR fragments containing the corresponding deletions.

The pCG-TPMV H Δ 32-IL-13 plasmid (Addgene; plasmid #163869), the pCG-TPMV F Δ 32 plasmid (Addgene; plasmid #163964), and the pCG-TPMV H Δ 32 plasmid (Addgene; plasmid #163963) are available from Addgene (Watertown, MA, USA).

Cell lines

HEK293T cells (ATCC CRL-3216; ATCC, Manassas, VA, USA) and HEK293 cells (catalog number 103; NIH AIDS Reagent Program, Germantown, MD, USA) were grown in Dulbecco's modified Eagle's medium (DMEM) containing high glucose (4.5 g/L), 2 mM L-glutamine, 10% heat-inactivated fetal bovine serum (FBS), 100 U/mL penicillin, and 100 μ g/mL streptomycin. Cell-culture reagents were purchased from Gibco (Thermo Fisher Scientific, Waltham, MA, USA).

Human U251 glioblastoma cells (National Cancer Institute [NCI], Frederick, MD, USA) were cultured in RPMI-1640 medium supplemented with 10% FBS, 25 mM HEPES, 0.1 mM nonessential amino acids, 2 mM glutamine, 1 mM sodium pyruvate, penicillin (100 U/mL), and streptomycin (100 μ g/mL) (all from Thermo Fisher Scientific).

The human NCI-H1299 NSCLC cell line (ATCC CRL-5803) (ATCC) was propagated in RPMI-1640 medium (ATCC) containing 10% heat-inactivated FBS, penicillin (100 U/mL), and streptomycin (100 μ g/mL).

NCI-H1299 GLuc cells were obtained by transduction using the NL(CMV)GLuc/CMV/WPRE Δ U3 LV vector.¹² Single-cell clones were obtained by limiting dilution, and clones with high GLuc activity were identified using the BioLux GLuc Assay Kit (New England Biolabs, Ipswich, MA, USA) as described by the manufacturer.

Vero- α His cells²⁵ were provided by Stephen Russell (Mayo Clinic, Rochester, MN, USA), and Vero cells were obtained from Alan Baer (US Food and Drug Administration/Center for Biologics Evaluation and Research [FDA/CBER]).

NIH 3T3 cells were provided by Carolyn Wilson (FDA/CBER).

LV vector production

LV vector production was carried out using 6-well plates, 15 cm dishes, or HYPERFlask cell-culture vessels (Corning, Lowell, MA, USA) as described.²⁷ For vector production in 6-well plates, 293T V6 cells (a clonal derivative of HEK293T cells with increased vector production capacity; W.O., unpublished data) were plated at 1×10^6 cells per well and transfected with 0.53 μ g of the pNL(CMV)TK2ALuc2/CMV/WPRE Δ U3 vector plasmid, 0.32 μ g of the pCD/NL-BH Δ 1 packaging plasmid, 0.76 μ g of the pCMV-Rev plasmid, 0.02 μ g of pCG-TPMV F, and 0.005 μ g of either the pCG-TPMV H-IL-13 or pCG-TPMV H plasmids. For 15-cm dishes and HYPER-Flask vessels, the number of cells and the quantities of the various plasmids were proportionally increased according to the cell-culture surface area. The cell-culture media were changed the day after transfection, and the vector-containing supernatants were harvested on the 3rd day (about 60 h) post-transfection, filtered through a 0.45- μ m pore-size filter (Millipore Sigma, Burlington, MA, USA), and stored at -80°C .

LV vectors for animal studies were produced using HYPERFlask vessels and concentrated using Mustang Q anion-exchange chromatography as described previously.^{26,27} Mustang Q XT Acrodisc 0.86 mL (MSTGXT25Q16) and 5 mL Mustang Q XT5 (XT5MSTGQPM6) units were purchased from Pall (Port Washington, NY, USA). Sartobind Q SingleSep nano 1 mL (92IEXQ42DN-11) and Sartobind Q nano 3 mL (96IEXQ42EUC11-A) were obtained from Sartorius Stedim Biotech (Göttingen, Germany).

Transfections were performed in DMEM supplemented with 10% FBS, 2.5 mM L-glutamine, 100 U/mL penicillin, and 100 μ g/mL streptomycin (all from Thermo Fisher Scientific). The media were removed the next day and replaced with an equal volume of Ultra-CULTURE medium (Lonza, Walkersville, MD, USA) supplemented with 2.5 mM L-glutamine (Thermo Fisher Scientific), 100 U/mL penicillin, and 100 μ g/mL streptomycin (Thermo Fisher Scientific). The vector-containing supernatants were filtered as described and loaded onto a 5-mL Mustang Q XT5 unit at a flow rate of 25 mL/min using an ÄKTA Pure 25 L1 chromatography system (Cytiva Life Sciences, Marlborough, MA, USA). The Acrodisc was then washed with 15 column volumes (CVs; 75 mL) of 150 mM NaCl in 25 mM Tris-HCl (pH 7.4), and vectors were eluted in 12 CV (60 mL) of 1.0 M NaCl in

25 mM Tris-HCl (pH 7.4). The eluted fraction was then further concentrated and desalted by centrifugation at $3,500 \times g$ using Centricon Plus-70 centrifugal filter units with Ultracel-PL membrane, 100 kDa (Millipore Sigma, Burlington, MA, USA), until a final volume of 1–2 mL was reached. The retentate was then diluted to 60 mL in Dulbecco's PBS (DPBS) and centrifuged as above until a final volume of 1–2 mL was reached. The desalted and concentrated retentates were then stored at -80°C . Vector stocks were titrated by qPCR using genomic DNA from transduced U251 cells using woodchuck hepatitis virus post-transcriptional regulatory element (WPRE)-specific primers.⁴⁵ Since vector-bearing, unmodified TPMV H glycoproteins cannot transduce cells, p24 levels were measured for both TPMV H Δ 32- and H Δ 32-IL-13-bearing vectors using Lenti-X GoStix Plus (Takara Bio USA, Mountain View, CA, USA), and vector inputs were normalized to p24 values.

Blocking vector uptake

Vector blocking was performed using a polyclonal goat anti-human IL-13R α 2 antibody (R&D Systems, Minneapolis, MN, USA) as described before.¹²

Determination of IL-13R α 2 levels

IL-13R α 2 levels on NCI-H1299 cells were determined indirectly by measuring the binding of anti-IL13-R α 2 antibody to the cell membrane as previously described.¹²

Animals and orthotopic lung cancer model

4- to 5-week-old female NSG mice were purchased from Jackson Laboratory (Bar Harbor, ME, USA). All animal procedures were performed by following the guidelines of Public Health Service Policy on Humane Care of Laboratory Animals and approved by the White Oak Consolidated Animal Program (WOC AP) Animal Care and Use Committee at CBER/FDA under protocol #2016-02. The WOC animal facilities are accredited by the Association for Assessment and Accreditation of Laboratory Animal Care International. All experiments were performed according to institutional guidelines. Animals were anesthetized with 2%–4% isoflurane for all experimental procedures.

After 1 week of acclimatization in the WOC animal facility, mice were grouped into control and experimental groups. Each group consisted of 3–6 animals. Animals were injected intrathoracically with NCI-H1299 cells, NCI-H1299 GLuc cells, or NCI-H1299 GLuc cells transduced *ex vivo* with the NL(CMV)TK2ALuc2/CMV/WPRE Δ U3 LV vector.

For intrathoracic cell implantation, 1.5×10^6 cells per animal were injected as previously described.²⁹

Evaluation of tumor formation using GLuc imaging

7 days after cell injection, engrafted animals were evaluated for tumor growth weekly over a period 3 to 4 weeks using bioluminescence imaging. For bioluminescence imaging, animals were anesthetized using 2%–4% isoflurane in an induction chamber. Coelenterazine

(Nanolight Technology, Pinetop, AZ, USA) (reconstituted in saline, 100 µg per animal) was injected i.v. via the tail vein of anesthetized animals. Within 1 min of injection, animals were imaged using a Caliper IVIS Lumina II bio-photometric imager (Caliper LifeSciences, Hopkinton, MA, USA).

Evaluation of vector distribution using FLuc imaging

Tumor-bearing mice were grouped based on tumor size determined by IVIS Lumina imaging to ensure relatively equal engraftment of the tumor cells per group. To evaluate vector targeting to IL-13R α 2-expressing tumor cells, mice were injected i.v. via the lateral tail vein with NL(CMV)TK2ALuc2/CMV/WPREΔU3 LV vectors bearing HΔ32-IL-13 and F glycoproteins (1.25×10^6 TU per mouse) or LV vectors bearing TPMV HΔ32 and F glycoproteins. 7 days post-injection, vector targeting was assessed by bioluminescence imaging of the animals following intraperitoneal (i.p.) injection of the FLuc substrate, D-luciferin (Caliper Lifesciences; 2 mg/animal), using a 1-mL syringe with a 27G needle according to a method described previously.⁴⁶ 12 min post D-luciferin injection, animals were anesthetized using 2%–4% isoflurane in an induction chamber. Anesthetized animals were immediately transferred to a Caliper IVIS Lumina II bio-photometric imager where images were acquired using IVIS Image software.

Histological assessment of tissue samples

Animals were sacrificed using CO₂ 48 h after imaging. Animals were immediately surgically opened for macroscopic examination of the injection site and organs. For histopathological examination, tissues including tumor cells were harvested and fixed in 10% neutral-buffered formalin for 48 h, embedded in paraffin, sectioned at 4–10 µm, and processed for routine H&E staining (HistoServ, Gaithersburg, MD, USA). Tissue slides were scanned at 10× and 20× using an Aperio AT2 digital slide scanner (Leica Biosystems, Buffalo Grove, IL, USA) from which representative microscopic images were captured.

For immunohistochemistry analysis, formalin-fixed tissues were dissected, and tissue fragments were immersed in 20% sucrose in PBS and kept overnight at 4°C for dehydration. After the 20% sucrose treatment, tissues were kept for 20 min in optimum cutting temperature (OCT) compound (Tissue Tek; Sakura Finetek USA, Torrance, CA, USA). The tissues were then transferred to cryomolds filled with OCT compound, held for 30 min in dry ice for freezing prior to storage at –80°C in freezing bags. On the day of sectioning, the OCT blocks were kept in the cryostat microtome for 20 to 30 min to adjust the temperature to –15°C to –20°C. The frozen tissues were cut at a thickness of 10 µm, and sections were mounted onto gelatin-coated histological slides.

Staining of sections with 4',6-diamidino-2-phenylindole (DAPI; Thermo Fisher Scientific) was carried out according to the manufacturer's instructions. To prepare the tissue sections for immunofluorescence, samples were incubated in anti-FLuc antibody (Thermo Fisher Scientific) and anti-FASN antibody (Sino Biologicals, Wayne,

PA, USA) followed by Alexa Fluor 488- and Alexa Fluor 594-labeled secondary antibodies (Thermo Fisher Scientific, Grand Island, NY, USA), respectively. The samples were rinsed with PBS twice before the slides were mounted with coverslips using mounting media for confocal microscopy. The slides were viewed using a Zeiss LSM 700 laser-scanning confocal microscope (Boston Microscopes, Wilmington, MA, USA).

Evaluation of vector distribution by PCR and ddPCR

Genomic DNA was extracted from tumors, lungs, and other internal organs such as liver and spleen using a DNeasy Blood & Tissue Kit (QIAGEN, Germantown, MD, USA) according to the manufacturer's instructions.

For regular PCR, a PCR primer set specific for the HSV-1 TK sequence was used. The primers included TRFYGfwd (5'-AGCAGAGGCCACAACAGA-3') and TRFYGrev (5'-CTCCCAGCAGCATGTTGGT-3'). The hRNaseP gene sequence⁴⁷ was used as an internal control.

For the PCR reaction, 300 ng of genomic DNA was used. PCR reactions were carried out using Taq DNA polymerase (Invitrogen, Carlsbad, CA, USA) with an initial denaturation step of 5 min at 95°C, followed by 30 cycles of denaturation (30 s, 95°C), annealing (30 s, 60°C), and extension (90 s, 72°C), as well as a final extension step of 10 min at 72°C.

Vector-specific TK gene sequences, human *PTGER2* gene sequences, and mouse *Ptger2* gene sequences³¹ were quantified with ddPCR. The primer/probe sequences and their associated concentrations are shown in Table S2. ddPCR was performed with the Bio-Rad QX200 ddPCR system according to standard protocols. Briefly, each ddPCR assay contained 2× BioRad ddPCR Mastermix, 900 nM of forward and reverse primers, 250 nM fluorescent probes, and 1 µL of tumor biopsy DNA product. Cycling conditions were 95°C for 10 min and then 50 cycles of 95°C for 30 s, 56°C annealing, and extension for 2 min. Post-cycling, a final enzyme de-activation, was performed at 98°C for 10 min. Data are shown as copies of the target per 1 µL of tumor biopsy DNA product.

SUPPLEMENTAL INFORMATION

Supplemental information can be found online at <https://doi.org/10.1016/j.omtm.2021.04.012>.

ACKNOWLEDGMENTS

We thank Nirjal Bhattarai and Syed Hussain for helpful comments on the manuscript. We thank Xiaohong Li and Park Jume, Division of Veterinary Services, FDA/CBER, for providing technical support during the animal experiments. The following was obtained through the NIH AIDS Reagent Program, Division of AIDS, NIAID, NIH: HEK293 cells from Dr. Andrew Rice. This work was supported by the Intramural Research Program of the Center for Biologics Evaluation and Research (CBER), US Food and Drug Administration. This project was supported in part by L.E.'s, A.T.'s, and P.L.'s appointment

to the Research Participation Program at CBER administered by the Oak Ridge Institute for Science and Education through the US Department of Education and the US Food and Drug Administration.

AUTHOR CONTRIBUTIONS

Study design, T.A., W.O., and J.R.; performed experiments, T.A., M.P.M., L.E., P.L., and W.O.; data analysis, T.A., A.K., A.T., K.T., and J.R.; writing – original draft, T.A.; writing – review & editing, J.R., A.T., T.A., M.P.M., A.K., and P.L. All authors reviewed the manuscript.

DECLARATION OF INTERESTS

The authors declare no competing interests.

REFERENCES

1. Waehler, R., Russell, S.J., and Curiel, D.T. (2007). Engineering targeted viral vectors for gene therapy. *Nat. Rev. Genet.* 8, 573–587.
2. Frecha, C., Szécsi, J., Cosset, F.L., and Verhoeven, E. (2008). Strategies for targeting lentiviral vectors. *Curr. Gene Ther.* 8, 449–460.
3. Cronin, J., Zhang, X.Y., and Reiser, J. (2005). Altering the tropism of lentiviral vectors through pseudotyping. *Curr. Gene Ther.* 5, 387–398.
4. Bischof, D., and Cornetta, K. (2010). Flexibility in cell targeting by pseudotyping lentiviral vectors. *Methods Mol. Biol.* 614, 53–68.
5. Lévy, C., Verhoeven, E., and Cosset, F.L. (2015). Surface engineering of lentiviral vectors for gene transfer into gene therapy target cells. *Curr. Opin. Pharmacol.* 24, 79–85.
6. Buchholz, C.J., Friedel, T., and Büning, H. (2015). Surface-Engineered Viral Vectors for Selective and Cell Type-Specific Gene Delivery. *Trends Biotechnol.* 33, 777–790.
7. Frank, A.M., and Buchholz, C.J. (2018). Surface-Engineered Lentiviral Vectors for Selective Gene Transfer into Subtypes of Lymphocytes. *Mol. Ther. Methods Clin. Dev.* 12, 19–31.
8. Yanagi, Y., Takeda, M., and Ohno, S. (2006). Measles virus: cellular receptors, tropism and pathogenesis. *J. Gen. Virol.* 87, 2767–2779.
9. Cattaneo, R. (2010). Paramyxovirus entry and targeted vectors for cancer therapy. *PLoS Pathog.* 6, e1000973.
10. Mühlebach, M.D., Mateo, M., Sinn, P.L., Prüfer, S., Uhlig, K.M., Leonard, V.H., Navaratnarajah, C.K., Frenzke, M., Wong, X.X., Sawatsky, B., et al. (2011). Adherens junction protein nectin-4 is the epithelial receptor for measles virus. *Nature* 480, 530–533.
11. Funke, S., Maisner, A., Mühlebach, M.D., Koehl, U., Grez, M., Cattaneo, R., Cichutek, K., and Buchholz, C.J. (2008). Targeted cell entry of lentiviral vectors. *Mol. Ther.* 16, 1427–1436.
12. Ou, W., Marino, M.P., Suzuki, A., Joshi, B., Husain, S.R., Maisner, A., Galanis, E., Puri, R.K., and Reiser, J. (2012). Specific targeting of human interleukin (IL)-13 receptor $\alpha 2$ -positive cells with lentiviral vectors displaying IL-13. *Hum. Gene Ther. Methods* 23, 137–147.
13. Anliker, B., Abel, T., Kneissl, S., Hlavaty, J., Caputi, A., Brynza, J., Schneider, I.C., Münch, R.C., Petznek, H., Kontermann, R.E., et al. (2010). Specific gene transfer to neurons, endothelial cells and hematopoietic progenitors with lentiviral vectors. *Nat. Methods* 7, 929–935.
14. Münch, R.C., Mühlebach, M.D., Schaser, T., Kneissl, S., Jost, C., Plückthun, A., Cichutek, K., and Buchholz, C.J. (2011). DARPins: an efficient targeting domain for lentiviral vectors. *Mol. Ther.* 19, 686–693.
15. Leber, M.F., Neault, S., Jirovec, E., Barkley, R., Said, A., Bell, J.C., and Ungerechts, G. (2020). Engineering and combining oncolytic measles virus for cancer therapy. *Cytokine Growth Factor Rev.* 56, 39–48.
16. Tidona, C.A., Kurz, H.W., Gelderblom, H.R., and Darai, G. (1999). Isolation and molecular characterization of a novel cytopathogenic paramyxovirus from tree shrews. *Virology* 258, 425–434.
17. Springfield, C., Darai, G., and Cattaneo, R. (2005). Characterization of the Tupaia rhabdovirus genome reveals a long open reading frame overlapping with P and a novel gene encoding a small hydrophobic protein. *J. Virol.* 79, 6781–6790.
18. Hudacek, A.W., Navaratnarajah, C.K., and Cattaneo, R. (2013). Development of measles virus-based shielded oncolytic vectors: suitability of other paramyxovirus glycoproteins. *Cancer Gene Ther.* 20, 109–116.
19. Springfield, C., von Messling, V., Tidona, C.A., Darai, G., and Cattaneo, R. (2005). Envelope targeting: hemagglutinin attachment specificity rather than fusion protein cleavage-activation restricts Tupaia paramyxovirus tropism. *J. Virol.* 79, 10155–10163.
20. Engeland, C.E., Bossow, S., Hudacek, A.W., Hoyler, B., Förster, J., Veinalde, R., Jäger, D., Cattaneo, R., Ungerechts, G., and Springfield, C. (2017). A Tupaia paramyxovirus vector system for targeting and transgene expression. *J. Gen. Virol.* 98, 2248–2257.
21. Enkirch, T., Kneissl, S., Hoyler, B., Ungerechts, G., Stremmel, W., Buchholz, C.J., and Springfield, C. (2013). Targeted lentiviral vectors pseudotyped with the Tupaia paramyxovirus glycoproteins. *Gene Ther.* 20, 16–23.
22. Lupardus, P.J., Birnbaum, M.E., and Garcia, K.C. (2010). Molecular basis for shared cytokine recognition revealed in the structure of an unusually high affinity complex between IL-13 and IL-13R $\alpha 2$. *Structure* 18, 332–342.
23. Suzuki, A., Leland, P., Joshi, B.H., and Puri, R.K. (2015). Targeting of IL-4 and IL-13 receptors for cancer therapy. *Cytokine* 75, 79–88.
24. Xie, M., Wu, X.J., Zhang, J.J., and He, C.S. (2015). IL-13 receptor $\alpha 2$ is a negative prognostic factor in human lung cancer and stimulates lung cancer growth in mice. *Oncotarget* 6, 32902–32913.
25. Nakamura, T., Peng, K.W., Vongpunswad, S., Harvey, M., Mizuguchi, H., Hayakawa, T., Cattaneo, R., and Russell, S.J. (2004). Antibody-targeted cell fusion. *Nat. Biotechnol.* 22, 331–336.
26. Kutner, R.H., Puthli, S., Marino, M.P., and Reiser, J. (2009). Simplified production and concentration of HIV-1-based lentiviral vectors using HYPERFlask vessels and anion exchange membrane chromatography. *BMC Biotechnol.* 9, 10.
27. Marino, M.P., Panigaj, M., Ou, W., Manirarora, J., Wei, C.H., and Reiser, J. (2015). A scalable method to concentrate lentiviral vectors pseudotyped with measles virus glycoproteins. *Gene Ther.* 22, 280–285.
28. Onn, A., Isobe, T., Itasaka, S., Wu, W., O'Reilly, M.S., Ki Hong, W., Fidler, I.J., and Herbst, R.S. (2003). Development of an orthotopic model to study the biology and therapy of primary human lung cancer in nude mice. *Clin. Cancer Res.* 9, 5532–5539.
29. Eldridge, L., Moldobaeva, A., Zhong, Q., Jenkins, J., Snyder, M., Brown, R.H., Mitzner, W., and Wagner, E.M. (2016). Bronchial Artery Angiogenesis Drives Lung Tumor Growth. *Cancer Res.* 76, 5962–5969.
30. Black, M.E., Kokoris, M.S., and Sabo, P. (2001). Herpes simplex virus-1 thymidine kinase mutants created by semi-random sequence mutagenesis improve prodrug-mediated tumor cell killing. *Cancer Res.* 61, 3022–3026.
31. Alcoser, S.Y., Kimmel, D.J., Borgel, S.D., Carter, J.P., Dougherty, K.M., and Hollingshead, M.G. (2011). Real-time PCR-based assay to quantify the relative amount of human and mouse tissue present in tumor xenografts. *BMC Biotechnol.* 11, 124.
32. Milone, M.C., and O'Doherty, U. (2018). Clinical use of lentiviral vectors. *Leukemia* 32, 1529–1541.
33. Naldini, L. (2019). Genetic engineering of hematopoiesis: current stage of clinical translation and future perspectives. *EMBO Mol. Med.* 11, e9958.
34. Liu, Y., Chen, X., Han, W., and Zhang, Y. (2017). Tisagenlecleucel, an approved anti-CD19 chimeric antigen receptor T-cell therapy for the treatment of leukemia. *Drugs Today (Barc)* 53, 597–608.
35. Schuessler-Lenz, M., Enzmann, H., and Vamvakas, S. (2020). Regulators' Advice Can Make a Difference: European Medicines Agency Approval of Zynteglo for Beta Thalassemia. *Clin. Pharmacol. Ther.* 107, 492–494.
36. Abramson, J.S., Palomba, M.L., Gordon, L.I., Lunning, M.A., Wang, M., Arnason, J., Mehta, A., Purev, E., Maloney, D.G., Andreadis, C., et al. (2020). Lisocabtagene marelcel for patients with relapsed or refractory large B-cell lymphomas (TRANSCEND NHL 001): a multicentre seamless design study. *Lancet* 396, 839–852.

37. Munshi, N.C., Anderson, L.D., Jr., Shah, N., Madduri, D., Berdeja, J., Lonial, S., Raje, N., Lin, Y., Siegel, D., Oriol, A., et al. (2021). Idecabtagene Vicleucel in Relapsed and Refractory Multiple Myeloma. *N. Engl. J. Med.* 384, 705–716.
38. Cavalieri, V., Baiamonte, E., and Lo Iacono, M. (2018). Non-Primate Lentiviral Vectors and Their Applications in Gene Therapy for Ocular Disorders. *Viruses* 10, 316.
39. Somaiah, N., Block, M.S., Kim, J.W., Shapiro, G.I., Do, K.T., Hwu, P., Eder, J.P., Jones, R.L., Lu, H., Ter Meulen, J.H., et al. (2019). First-in-Class, First-in-Human Study Evaluating LV305, a Dendritic-Cell Tropic Lentiviral Vector, in Sarcoma and Other Solid Tumors Expressing NY-ESO-1. *Clin. Cancer Res.* 25, 5808–5817.
40. Bender, R.R., Muth, A., Schneider, I.C., Friedel, T., Hartmann, J., Plückthun, A., Maisner, A., and Buchholz, C.J. (2016). Receptor-Targeted Nipah Virus Glycoproteins Improve Cell-Type Selective Gene Delivery and Reveal a Preference for Membrane-Proximal Cell Attachment. *PLoS Pathog.* 12, e1005641.
41. Friedel, T., Hanisch, L.J., Muth, A., Honegger, A., Abken, H., Plückthun, A., Buchholz, C.J., and Schneider, I.C. (2015). Receptor-targeted lentiviral vectors are exceptionally sensitive toward the biophysical properties of the displayed single-chain Fv. *Protein Eng. Des. Sel.* 28, 93–106.
42. Abel, T., El Filali, E., Waern, J., Schneider, I.C., Yuan, Q., Münch, R.C., Hick, M., Warnecke, G., Madrahimov, N., Kontermann, R.E., et al. (2013). Specific gene delivery to liver sinusoidal and artery endothelial cells. *Blood* 122, 2030–2038.
43. Zhou, Q., Uhlig, K.M., Muth, A., Kimpel, J., Lévy, C., Münch, R.C., Seifried, J., Pfeiffer, A., Trkola, A., Coulibaly, C., et al. (2015). Exclusive Transduction of Human CD4+ T Cells upon Systemic Delivery of CD4-Targeted Lentiviral Vectors. *J. Immunol.* 195, 2493–2501.
44. Agarwal, S., Hanauer, J.D.S., Frank, A.M., Riechert, V., Thalheimer, F.B., and Buchholz, C.J. (2020). In Vivo Generation of CAR T Cells Selectively in Human CD4+ Lymphocytes. *Mol. Ther.* 28, 1783–1794.
45. Kutner, R.H., Zhang, X.Y., and Reiser, J. (2009). Production, concentration and titration of pseudotyped HIV-1-based lentiviral vectors. *Nat. Protoc.* 4, 495–505.
46. Wu, J.C., Sundaresan, G., Iyer, M., and Gambhir, S.S. (2001). Noninvasive optical imaging of firefly luciferase reporter gene expression in skeletal muscles of living mice. *Mol. Ther.* 4, 297–306.
47. Serruya, R., Orlovetskie, N., Reiner, R., Dehtiar-Zilber, Y., Wesolowski, D., Altman, S., and Jarrous, N. (2015). Human RNase P ribonucleoprotein is required for formation of initiation complexes of RNA polymerase III. *Nucleic Acids Res.* 43, 5442–5450.